

Quantitative Comparison of Deformable Models in Range Segmentation

Khaldi Amine, Merouani Hayet Farida

*Department of Computer Sciences, Badji Mokhtar University, Laboratory of LRI, BP12.Sidi Amar,
23000 Annaba, Algeria
Emails: Tiva.amine@live.fr Merouani_hayet@yahoo.fr*

Abstract: *In this paper we segment range images by applying three deformable models (the classical Active Contour, the adaptive active contour and the Level Set method). These three methods are used to segment images with planar and curved surface scenes. Then the numerical results obtained are compared in order to find the best technique of deformable models adapted to segmentation of range images. Despite of the good experimental results on simple objects, we have noted that the adaptive and classical snake methods have a few limitations and cannot detect discontinuities in curvatures and some items do not always converge. However, the level set method is very efficient for segmenting range images with curvature and complex forms.*

Keywords: *Range image, segmentation, deformable model, active contour, snake, level set.*

1. Introduction

The segmentation process is perhaps the most important step in image analysis. Its performance directly affects the subsequent processing steps of the image and significantly determines the interpretation of the resulting image [1]. The two main

difficulties of the range segmentation problem are its nature and the lack of definition of correct segmentation. Perhaps due to these defects, plenty of segmentation algorithms have been proposed in literature [2]. Range image segmentation is the process of dividing an image into areas that are associated with specific objects in a scene; these objects can be identified in a range image as patches that are relatively uniform in surface shape or range value. Range segmentation [3] has been used most frequently in 3D object recognition tasks and considerable progress has been achieved. However, the recognition of a real world scene based on a single range image is a difficult task. This is due to the nature of the scene which may include objects [4] with irregular shapes that have no clearly defined geometry, objects viewed from any direction and objects with self-occlusion or partially occluded by other objects. The purpose in this paper is to apply deformable models to segment range images, using three active contours (a classical active contour, a classical improved active contour called “adaptive active contour” and the Level set method). Through this application we intend to consider the behaviour of the active contours on range images, and will later try to analyze the segmentation results in order to define which algorithm is the most suitable one for these images. The remainder of the paper is organized as follows. Section 2 describes the range image and some examples of range sensors. In Section 3 an overview of the adaptive contour used and the level set method is presented. The experimental results are discussed in Section 4, and finally, conclusions from the work done are drawn and further research is suggested.

2. Range image

2.1. Definition

A range image is a two-dimensional array of 3D positions [5], checking the spatial coherence property, each component of this matrix represents the distance between a reference point (the sensor) and a point in the field of vision of the sensor (camera, video camera). It is the equivalent of a video image wherein the gray level of each pixel (x, y) would be replaced by an altitude z (2.5D is an intermediate case between the 2D and 3D not fractal dimensions). The feature of this type of data thus lies essentially in its grid structure (x, y) and in its ability to describe the scene graph as a function $z = f(x, y)$. The term range (range picture element) refers to an element of the array. The range images provide geometric information about the object, independent of the position, direction and intensity of the light sources illuminating the scene, or of the reflectance properties of the object. For these reasons the range images play a very important role in image understanding, in three-dimensional object reconstruction, autonomous navigation, medical diagnosis, etc.

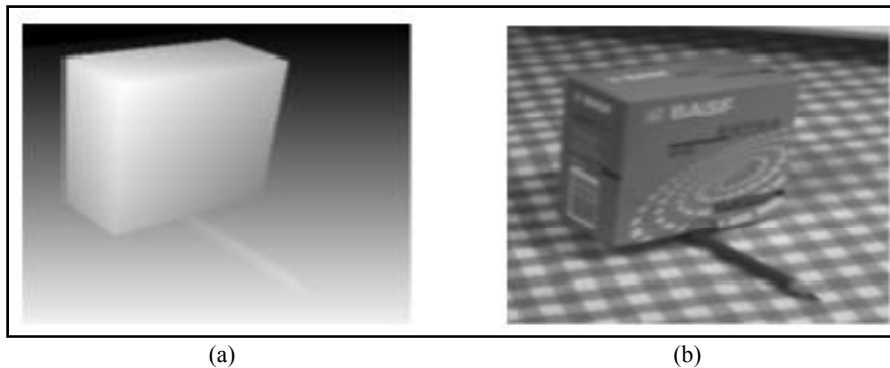


Fig. 1. Range image example: original intensity image (a); corresponding range image (b)

2.2. Depth of the range image

The depth is the distance between the visible surface of an object in a scene and the camera. It is a useful indicator for the calculation of the point's coordinates belonging to this surface in a three-dimensional space reference. Many methods have been developed [6] to obtain 3D coordinates of objects using range images, and they all exploit the changes in the acquisition parameters of the system taken. These parameters acquisition system or light environment provides information essential to establish the relationship between the image and the actual scene.

2.3. Range imaging sensor

The range imaging sensors collect 3D coordinate data from the reflective surfaces of the objects in a scene. They (the range imaging sensors) may be classified as being either active, or passive [7]. The active sensors project energy onto a scene and measure the portion of the energy that is reflected. Radar, sonar and laser ranging systems are examples of active sensors. The passive sensors operate using the existing environmental conditions; an aerial stereo imaging system is a good example. Laser ranging digital cameras have emerged as premier devices useful in a broad class of 3D computer vision applications due to their spatial accuracy, resolution, ratio cost/performance. Recently, the range image sensors are evolving continuously, allowing nowadays digitizing of a full scene with high resolution in a short time. Thus, the algorithms and techniques developed to process range images have to develop with the same dynamism to enforce the processing of the whole information rapidly.

2.3.1. Flying laser range sensor

The Flying Laser Range Sensor (FLRS) was developed to measure large-scale objects from the air by using a balloon as a base rather than constructing scaffolds. With respect to the measurement principle, the passive stereopsis method could capture images (Fig. 2) without the influence of the balloon motion. The laser radar method [8] is suitable for outdoor measurement of large objects.



Fig. 2. FLRS result: the object for the experiment (a); the range data obtained (b)

2.3.2. Imaging radar

A second method for range imaging is the imaging radar [9]. In a time-of-flight pulsed radar the distance to the object is computed by calculating the time difference between the transmitted and received electromagnetic pulse, the depth information is obtained by detecting the phase difference between the transmitted and received waves. Several commercial laser beam imaging systems are built using these principles.

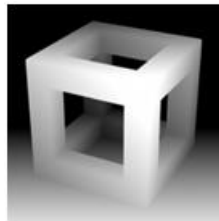


Fig. 3. A range image acquired by a time-of-flight pulsed radar

2.3.3. Stereo camera

A stereo camera [10] is a type of camera with two or more lenses with a separate image sensor or film frame for each lens. This technique allows the camera to simulate the human binocular vision, and enables it to capture three-dimensional images (this process is known as stereo photography). The stereo cameras may be used for making 3D pictures for movies and for range imaging. The stereo cameras are sometimes mounted in cars to detect the lane's width and the proximity of an object on the road.



Fig. 4. A range image acquired by a stereo camera

3. Developments

The proposed algorithms are implemented in Java NetBeans 7.21 which is a RAD (Rapid Application Development), an open-source Integrated Development Environment for software developers designed by Sun for creating applications and a GUI with all the tools needed to create a professional desktop, enterprise, web and mobile applications based on Java language. NetBeans IDE is easy to install and use straight out of the box and it runs on many platforms, including Windows, Linux, Mac OS X and Solaris.

3.1. Pre-processing

The contour of the objects in a scene is affected by noisy pixels which are caused by the detector noise, quantization and calibration errors and which often lead to unreliable image segmentation results [11]. Range images with noise will hamper the recognition and positioning of the target. In this study, in order to alleviate the effects of any noise present, the image is filtered by a Floyd & Steinberg filter which improves the overall perception of the range image and avoids the exclusion of low intensity areas as given in Fig. 5a.

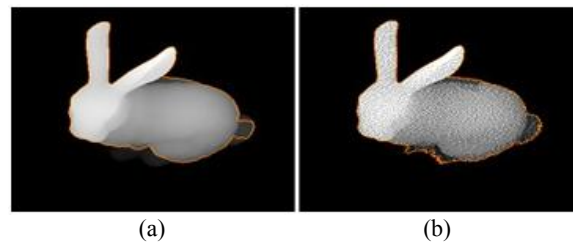


Fig. 5. Segmented image: without dithering (a); using Floyd & Steinberg dithering (b)

The Floyd-Steinberg dithering algorithm [12] is based on error dispersion. For each point in the image we find the closest color available. We calculate the difference between the value in the image and the color we have, then we divide these error values and distribute them over the neighboring pixels which have not been visited yet. When we get to these later pixels, we just add the errors distributed from the earlier ones and clip the values to the allowed range if needed. We start our experiment with Sobel, Canny and Prewitt dithering which are traditionally used in range segmentation, but as it can be seen in Fig. 6, these three filters are not adequate for our segmentation method (Snake).

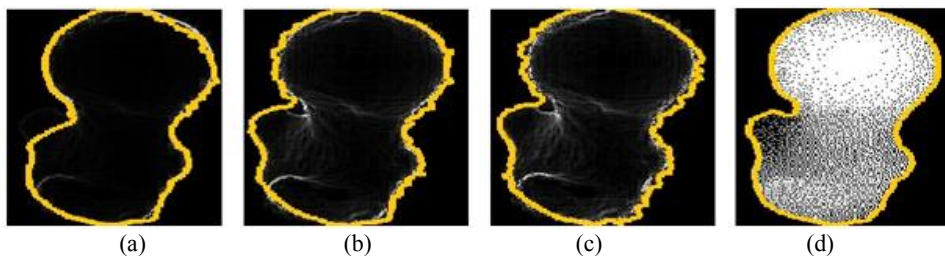


Fig. 6. Segmented image: Canny (a); Sobel (b); prewitt (c); Floyd & Steinberg (d)

3.2. The classic snake method

The classic snake we use is a parametric curve “C” that will be attracted to areas with strong gradients (where the norm of the gradient of a point will be very high). The principle is to place in the image an initial contour which is then deformed under the action of several energies. This maneuver needs two energies – internal energy and external energy

- Internal energy: The internal energy will depend on the derivatives of first and second order of the parametric curve representing the snake. This energy corresponds to the shape and curve characteristics, such as curvature and length.
- The external energy is related to the image and its properties and characteristics, such as the presence of edges or noise. It ensures that the snake is on the edges of the image by maximizing the amount of the standard gradient throughout the curve and thus minimizing its opposite.

The initial contour is first placed in the center of the image in a circle; the movement and evolution of this model is through iterations of the algorithm to minimize the total energy. For each point P of the active contour energy, a function E is calculated for every point n belonging to the neighborhood of P . The point P_0 , characterized by minimum energy E_0 is then chosen to replace P if $E > E_0$. Otherwise, the contour point P is not changed. This mechanism is repeated until convergence (when the contour obtained at iteration t is identical to that obtained at iteration $t + 1$).

3.3. The Level Set method

The Level Set technique is an important category of modern image segmentation techniques based on Partial Differential Equations (PDE). After progressive evaluation of the differences among neighboring pixels to find the object boundaries, ideally, the algorithm will converge to the boundary of the object where the differences are the highest. The outstanding characteristics of the level set methods are that the contours can split or merge as the topology of the level set function changes. This method [13] can detect more than one boundary simultaneously by placing multiple initial contours, but the convergence speed will be slower than in other segmentation methods.

The idea is to start with a closed curve and allow it move perpendicular to itself at a prescribed speed. We describe this curve by using an explicit parametric form (as the one used in snakes), but it causes difficulties when the curves have to undergo splitting or merging. To address this difficulty during the evolution to the desired shape, the implicit active contour takes the original interface and embeds it in a higher dimensional scalar function, defined over the entire image. The interface is represented implicitly as the zero-th level set (or contour) of this scalar function over the rest of the image space. This level set function is a signed distance function from the zero-th level set. This gives a closed curve C_0 . If the pixel lies on the curve, the function will be zero; otherwise, it is the signed minimum distance from the pixel to the curve (the distance is negative for pixels inside C_0 and positive for pixels outside C_0). The function varies with time and space and is evolved using a

Partial Differential Equation (PDE) containing terms that are either hyperbolic or parabolic; the evolution of our function can be written as

$$(1) \quad \Psi_{t+1} + F|\nabla\Psi_t| = 0,$$

where F is the speed in the direct n normal to the curve. We consider the evolution of the function as it evolves in a direction normal to itself with a known speed F .

The speed F is composed of three terms, a term constant (similar to the force of inflation used in the deformable models), a term dependent on the curvature local at each point and a term dependent on the image (in our case, the edges of the image):

$$(2) \quad \psi_{n+1} = \psi_n - dt.k_1(x, y).(U_n - \varepsilon K).|\nabla\psi_n|, \quad \varepsilon \in [0, 1],$$

where U_n is the function defining the area or object to be searched, K is the local curvature at each point, k_1 is the stopping criterion.

A key challenge in the level set is the placement of the initial contour. Since the contour moves either inward or outward, the segmentation obtained is dependent on the initial placement of the contour points. We start with an initial contour centered on the image, the sign of the so called “balloon force” is changed to generate the necessary outward propagation of the initial contour. Then the signed distance function is calculated (the minimum distance from each pixel in the image to the prescribed initial contour). It is done by solving the Eikonal equation. The signed distance function can often lose the distance property. When the curve stops evolving near an edge and the zero level set is not exactly at the edge, the distance function is re-initialized.

3.4. Adaptive active contours

The technique of active contours [14] is based upon the utilization of deformable contours which conform to various object shapes and motions. Snakes provide an accurate location of the edges only if the initial contour is given sufficiently near to the edges, because they only use the local information along the contour. That is why estimating the proper position of the initial contours without prior knowledge is a difficult problem. The adaptive active contour mixes two classical approaches of deformable models, deformable curves and classical active contours. In deformable curves formulation, a curve is submitted to a deformation vector field and only the normal component of the deformation vector acts on the shape of the curve. This method, based on deformation along normals, causes the model attraction to the nearest edges found perpendicularly to the model, which in the case of infoldings are located inside cavities. The final displacement results from a compromise between the complete displacement towards the nearest contour along the normal and the satisfaction of the geometrical constraints incorporated into the internal energy. The snake is a list of points and each point is attracted towards the nearest edge along the normal of this point. The Canny-Deriche operator is used to detect the edges. Starting from the position of a point we search along the normal for the nearest pixel having a gradient magnitude above a specified threshold. The segmentation of an image by an adaptive snake operates through an energy functional, controlling the deformation of an initial contour curve under the

influence of internal and external forces achieving a minimum energy state at high gradient locations. The energy functional for the active contour models is expressed as (3)

$$(3) \quad E(C) = \alpha \int_0^1 |C'(s)|^2 ds + \beta \int_0^1 |C''(s)| ds - \lambda \int_0^1 |\nabla I(C(s))|^2 ds.$$

The first two terms (α , β) control the rigidity and elasticity of the contour (defining the internal energy of the deformable object), while the last term attracts the model to high gradient locations in the image (defining the external energy of the model). We denote by $C(s) = (x(s), y(s))$ (the arc length being $s \in [0, 1]$) the current point of the contour C .

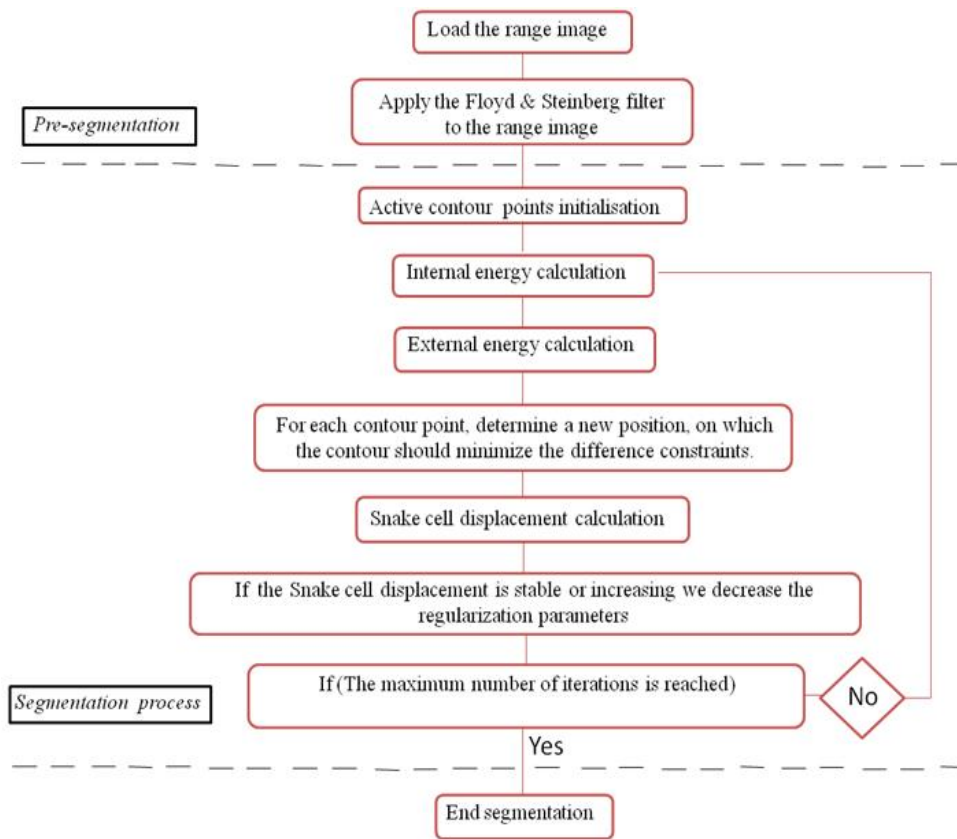


Fig. 7. Adaptive snake algorithm

We define this snake model as closed 2D contour elements. These nodes are associated with the time variation depending on the set of nodes connected in series. The snake is initialized by a position and a shape that significantly differ from that of the structure of interest. Initially, the regularization parameters are given high values in order to guarantee the model smoothness and to capture the overall shape of the object. At each step the average point displacement is calculated. If the displacement is stable or increasing, the regularization parameters are decreased for the next iteration (it allows the snake to progressively enter small infoldings).

4. Experimental results

In this section we describe the results of the experiments of segmentation using the adaptive snake and the level set methods. After that the segmentation results obtained are compared with the results of our previous classic snake algorithm. We are interested in understanding what benefits are obtained by the level set and deformable curves approach. The performance analysis has been conducted on a standard PC with an Intel(R), 2.20 GHz Processor, with 1 GB RAM. In order to evaluate the quality of the methods proposed we have used about 82 real range images from Stuttgart database. This database contains a collection of synthetic range images taken from high-resolution polygonal models available on the web. Six of these models (07_Deoflach, 08_Deorund, 15_Mole, 24_Kroete, 28_Ente, 29_Schwein) were reconstructed from real range scans at Stuttgart lab (they can also be downloaded from <http://range.informatik.uni-stuttgart.de/htdocs/html/>). To illustrate the experimental results, we present a set of images and a table. We differentiate between two categories of images (simple images and images with curvature). Fig. 8 shows the segmentation results using the implicit active contour, the adaptive snake and the level set approach on simple images.

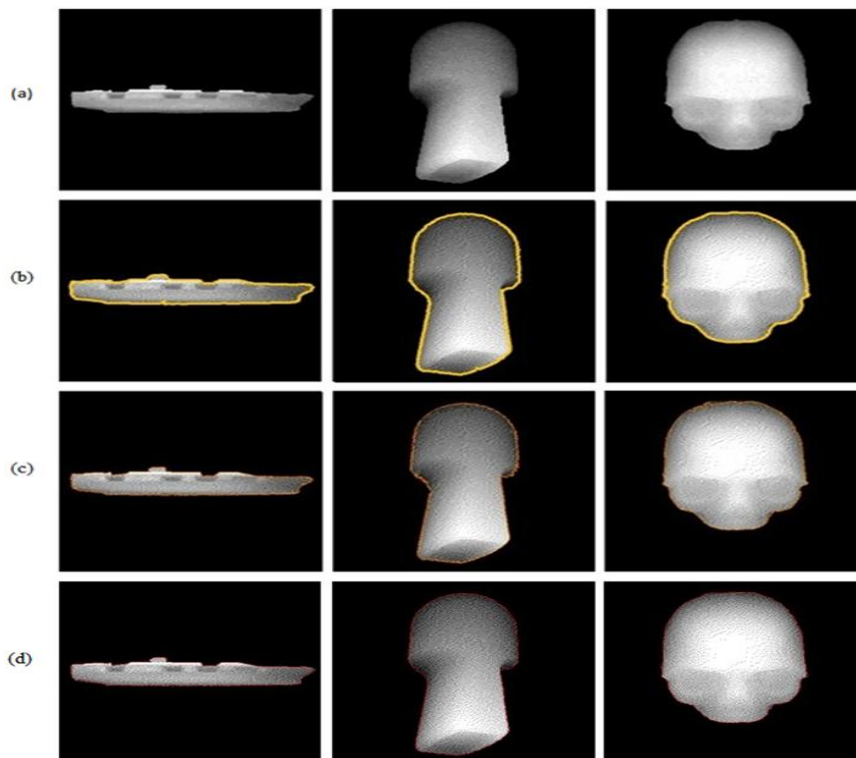


Fig. 8. Simple range image segmentation: the range image (a); segmentation obtained by applying the classic snake algorithm (b); segmentation results using the Level Set method (c); segmentation obtained using adaptive snake algorithm (d)

As seen in Fig. 8, the classic snake algorithm and the adaptive snake offer perfect segmentation for the simple images. However, the results of segmentations obtained for range images with cavities are not complete for the adaptive and classic snakes. The two snakes' methods cannot segment very thin and complex structures, such as the ones presented in Fig. 9 and do not enter into cavities. The limitations of the edge-based energy terms are well known. The models often either fail to lock on to weak edges, or become distracted from the feature of interest by stronger, but less interesting edges.

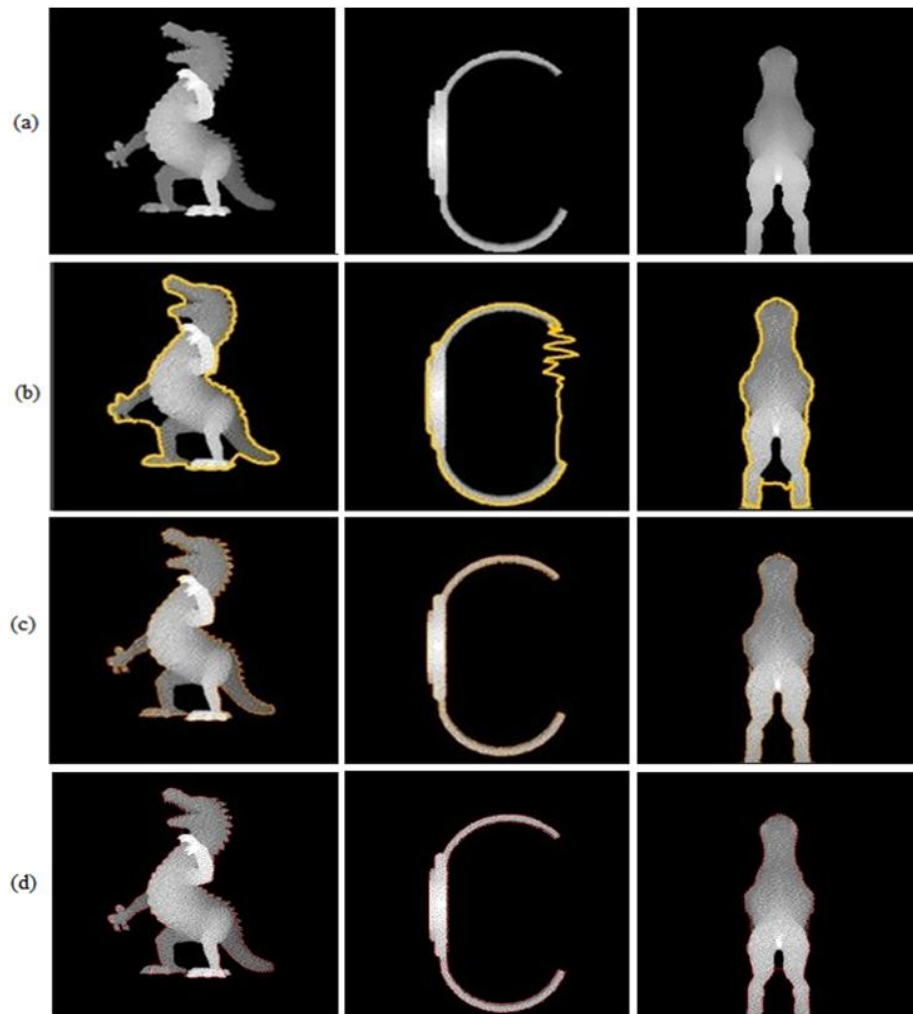


Fig. 9. Range image with curvature segmentation: the range image (a); segmentation obtained using the classic snake algorithm (b); segmentation results using the Level Set method (c); (d) segmentation obtained using the adaptive snake algorithm

Fig. 9 shows the segmentation results using the implicit active contour and the level set approach on the range images with cavity and as seen the level set

algorithm offers better segmentation results than the classic snake and the adaptive snake algorithms. In order to evaluate the three different segmentation methods, we have segmented the range images manually and developed a framework in C++ Builder that compares the contour point's position obtained, using the three methods to the position of the contour points in the reference segmentation. Then we calculate the percentage of pixels in right places.

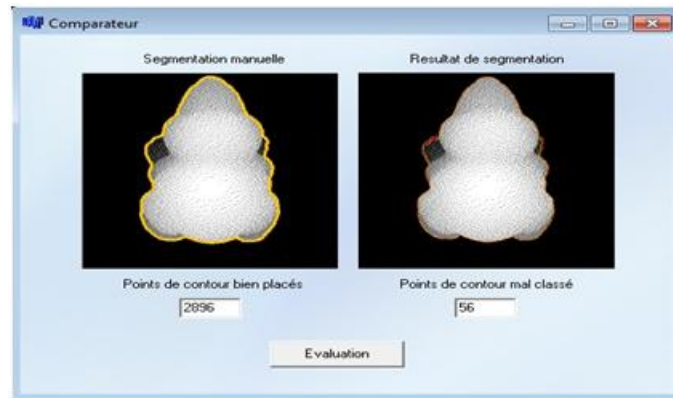


Fig. 10. Framework developed for the comparison

The rate of good segmentation was calculated for the 82 segmented images and those of the three techniques (Level set, Adaptive and Snake Classic Snake). The overall result (on average) is 96.01% of correct detection for images segmented via the algorithm Level sets, followed by the adaptive active contour algorithm (Fig. 11) with a rate of 95.17% . The classical active contour algorithm offers 82.60% of correct detection (which is less than the results obtained by the other two approaches).

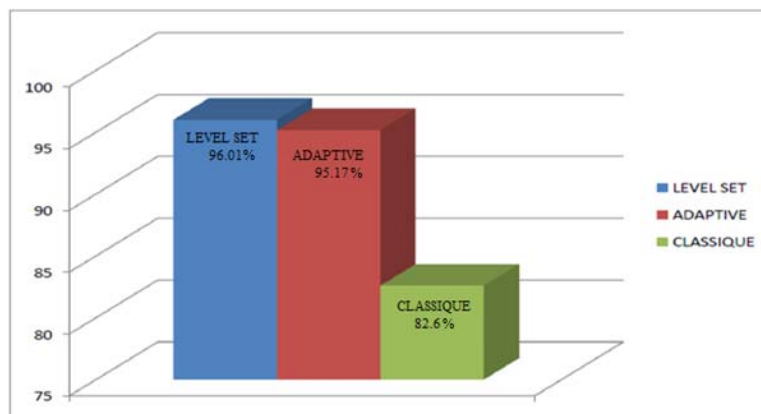


Fig. 11. Rate of good segmentation for each algorithm

We then analyzed separately the good segmentation rate for simple images (without cavities) and complex images having cavities for the three algorithms applied. We note that for simple images, the traditional active contour provides very

good results with 98% of good segmentation. Fig. 12 shows more in comparison to the adaptive active contours and the level set respectively – 94% and 96%. However, for images with deep cavities we note that the Level set and the adaptive snake provide good segmentation results (96% and 95.69%) in contrast to the classical snake (Fig. 13) that accounts only 67% of good segmentation.

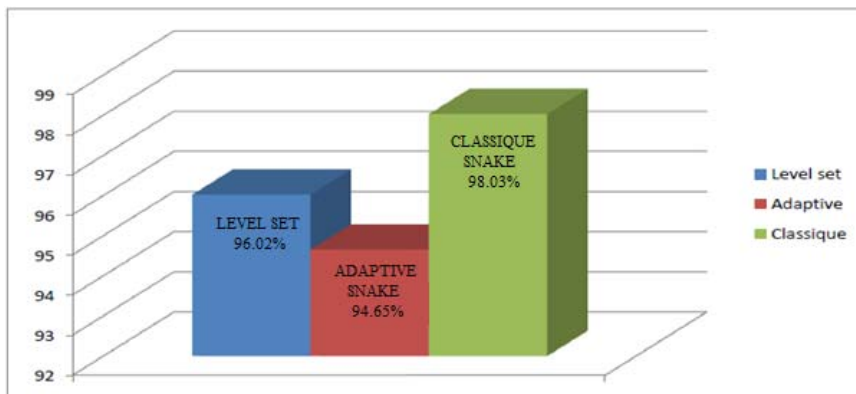


Fig. 12. Rate of good segmentation for simple images

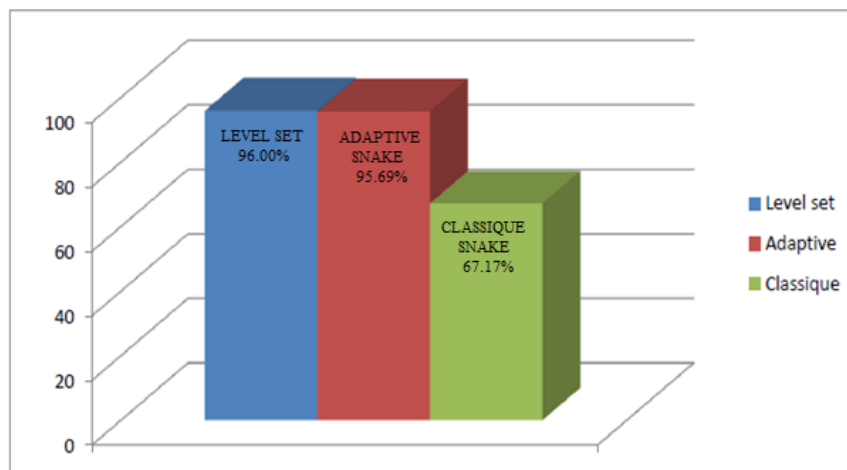


Fig. 13. Rate of good segmentation for complex images

We have analyzed the rate of good segmentation obtained and retained the best segmentation algorithm for each range image of our base (Fig. 14). We have discovered that the Level sets algorithm segments both simple images and complex images with cavities, and it has been selected as the best algorithm for 37 range images out of the 82 range images used. In analyzing the results of the classical and the adaptive active contour, they certainly offer good segmentation results for simple images, but they were retained only for 23 images out of the 82 images used.

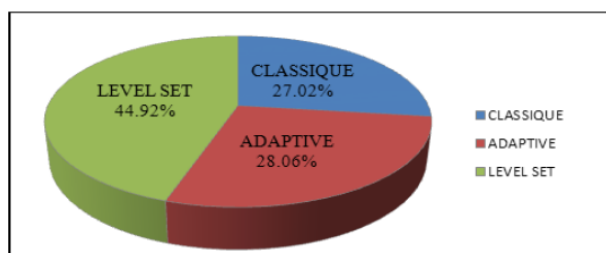


Fig. 14. The best algorithm selected for each image

We chose eight of these 82 results where the difference is greater than 3% (compared to the best segmentation rate). As seen from the results in Table 1, this confirms our visual comparison for images with cavities. The worst result obtained by the Level sets algorithm is the image “Pitt4” with 92.17% of correct detection. Unlike, the classic snake gives very poor results for images with cavity as seen in “Dinopet3” with a score of 76.48% and “Watch1” – 54.55% which is a significant difference compared to the other results obtained by the Level sets (96.16% and 97.05% respectively) and the adaptive snake (94.67% and 85.21% respectively).

Table 1. Percentage of good detection for the Snake, Level set and Adaptive active contours methods

Method	Fighter5	Agfa3	Pitbull3	Manta2	Dinopet3	Watch1	Pitt4	Kroete2
Snake	98.57%	99.19%	80.74%	89.96%	76.48%	54.55%	76.16%	85.18%
Level set	95.12%	95.18%	98.07%	97.44%	96.16%	97.05%	92.17%	95.01%
Adaptive	94.24%	98.70%	92.36%	96.05%	94.67%	85.21%	81.21%	97.89%

5. Conclusions

This paper discusses the use of a deformable model for an important low level computer vision problem, namely, range image segmentation. We have presented and compared three methods for edge detection applied to range images based on deformable models. As mentioned in the introduction, the motivation of our work was to apply two deformable models (Snake) which has never been done before in range segmentation. Despite the good experimental results on a simple object, the first method (Adaptive snake) proposed in this paper, has a few limitations and cannot detect discontinuities in curvatures. The adaptive active contours are very relevant in isolating regular convex shapes; however, they have some disadvantages. First, the function is not intrinsic and depends on the parameterization of the contour (the choice of constants is difficult). The snake provides accurate location of the edges only if the initial contour is given sufficiently near the edges because it uses only the local information along the contour (estimating the proper position of initial contours without prior knowledge is a difficult problem). The geometry of the object to be detected is not taken into account. Finally, the minimization of its functional shows terms that require calculation of the derivatives of order 4, which poses some problems in discretization and numerical instabilities. In the future we plan to extend this work by including geodesic and geometric active contours and evaluate them on real range images.

References

1. Khaldi, Amine, Hayet Merouani. An Active Contour for Range Image Segmentation. – An International Journal Signal & Image Processing, Vol. **3**, 2012, No 3, 17-29.
2. Merchan, P., A. S. Vasquez, A. Adan, S. Salamanca. 3D Scene Analysis from a Single Range Image through Occlusion Graphs. – Pattern Recognition Letters, Vol. **29**, 2008, 1105-1116.
3. Peng, Xiaoming, M. Bennamoun, A. S. Mian. A Training-Free Nose Tip Detection Method from Face Range Images. – Pattern Recognition, Vol. **44**, 2011, No 3, 544-558.
4. Mishima, Katsuaki, Tomohiro Yamada, Asuka Ohura, Toshio Sugahara. Production of a Range Image for Facial Motion Analysis: A Method for Analyzing Lip Motion. – Computerized Medical Imaging and Graphics, Vol. **30**, 2006, 53-59.
5. Coleman, S. A., Shanmugalingam Suganthan, B. W. Scotney. Gradient Operators for Feature Extraction and Characterization in Range Images. – Pattern Recognition Letters, Vol. **31**, 2010, 1028-1040.
6. Hernández, J., B. Marcotegui. Point Cloud Segmentation towards Urban Ground Modeling. – In: Proc. of 5th Workshop on Remote Sensing and Data Fusion over Urban Areas, Shangai, China, 2009.
7. Kohlhepp, P., D. Fischer, E. Hoffmann. Intrinsic Line Features and Contour Metric for Locating 3-D Objects in Sparse, Segmented Range Images. – Image and Vision Computing, Vol. **17**, 2009, 403-417.
8. Banno, A., T. Masuda, T. Oishi, K. Ikeuchi. Flying Laser Range Sensor for Large-Scale Site-Modeling and Its Applications in Bayon Digital Archival Project. – International Journal of Computer Vision, Vol. **78**, 2008, 207-222.
9. Miles, H., Lee Seungkyu, Cho Ouk, Horaud Radu. Time-of-Flight Cameras: Principles, Methods and Applications. – Springer Briefs in Computer Science. ISBN 978-1-4471-4657-5, 2012.
10. Kanga, Dong-Joong, Sung-Jo Lima, Jong-Eun Hab, Mun-Ho Jeong. A Detection Cell Using Multiple Points of a Rotating Triangle to Find Local Planar Regions from Stereo Depth Data. – Pattern Recognition Letters, Vol. **30**, 2009, No 5, 486-493.
11. Wang, Qi, Qi Li, Zhe Chen, Jianfeng Sun, Rui Yao. Range Image Noise Suppression in Laser Imaging System. – Optics and Laser Technology, Vol. **41**, 2009, 140-147.
12. Dagar, Anuja, Archana, Deepak Nandal. High Performance Computing Algorithm Applied in Floyd Steinberg Dithering. – International Journal of Computer Applications, Vol. **43**, April 2012, No 23, 0975-8887.
13. Peng, Daping, Barry Merriman, Stanley Osher, Hongkai Zhao, Myungjoo Kang. A PDE-Based Fast Local Level Set Method. – Journal of Computational Physics, No 155, 1999, 410-438.
14. Weeratunga, S. K., C. Kamath. An Investigation of Implicit Active Contours for Scientific Image Segmentation. – In: Proc. of Visual Communications and Image Processing Conference, San Jose, CA, January 2004, 18-22.